Lasers in Manufacturing Conference 2023

Analytical model for the calculation of the depth progress of V-shaped grooves obtained by laser ablation with ultrashort pulses

Daniel Holder[a,b,*], Rudolf Weber[a], Christian Hagenlocher[a], Thomas Graf[a]

[a]*Institut für Strahlwerkzeuge (IFSW), University of Stuttgart, Pfaffenwaldring 43, 70569 Stuttgart, Germany*
[b]*ARENA2036 Research Campus, Pfaffenwaldring 19, 70569 Stuttgart, Germany*

Abstract

The depth progress and the final depth of V-shaped grooves are described by an analytical model for laser ablation of metals with ultrashort laser pulses. The model assumes that the fluence absorbed along the walls is distributed with a linear increase from the edge to the tip of the groove. The depth progress of the machined groove is recursively calculated based on the depth increments induced by successive scans of the laser beam along the groove. Experimental results agree well with the calculated predictions in the case of titanium alloy and tungsten carbide and for different pulse energies, repetition rates, scanning speeds, and number of scans. This confirms the validity of the model and its assumptions, and highlights the model as a useful tool for estimating groove dimensions, optimizing of process windows for machining with high depth progress, and predicting the maximum achievable groove depth.

Keywords: laser ablation; grooves; ultrashort laser pulses; analytical model; depth progress

1. Introduction

The process of laser ablation with ultrashort laser pulses is highly versatile and finds widespread applications The dimensions of the ablated grooves, including the depth, width, and aspect ratio (depth/width), have a significant impact on the performance of the respective application. Predicting the achievable depth of the grooves or estimating the rate of depth progression during laser ablation remains challenging due to the complex interplay of various laser and scanning parameters, as well as material properties, including the depth of the groove itself. To address this, a simplified analytical model for predicting

* Corresponding author. Tel.: +40 711 685 69740; fax: +49 711 685 82113.
E-mail address: daniel.holder@ifsw.uni-stuttgart.de.

the depth progress in laser machining of V-shaped grooves was derived by Holder et al., 2022 and is shortly introduced here. The model is experimentally verified for different materials and various laser parameters, including pulse energy, repetition rate, scanning speed, and number of scans.

2. Analytical model for the prediction of the depth and width of laser ablated grooves

In analogy to the model presented by Holder et al., 2021 for percussion drilling of conical microholes, an analytical and recursive model for calculating the depth progress of laser machined V-shaped grooves in metals was derived. Only the basic principle and the assumptions of the model are described in the following. The equations and detailed information about the model can be found in Holder et al., 2022. Fig 1 sketches the cross section in the *y*-*z*-plane perpendicular to the scanning direction *x* including the quantities which are considered by the model. The assumption of a V-shaped grooves coincides with the assumptions of an increased absorptance by multiple reflections, which leads to a linear increase of the absorbed irradiation from the sample surface towards the tip of the groove, as described in detail by Holder et al., 2022.

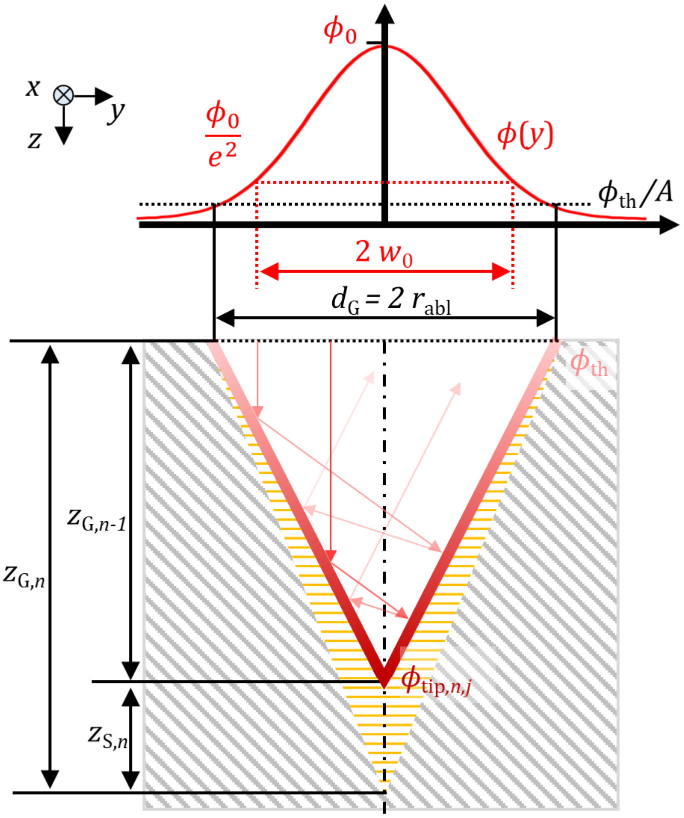

Fig. 1. V-shaped groove machined by a pulsed laser beam which is scanned along the *x*-axis. The Gaussian distribution of the fluence of the individual laser pulses is shown by the red curve. The width of the groove $d_G = 2\,r_{abl}$ corresponds to two times the ablation radius r_{abl}. The red arrows within the groove represent multiple reflected rays. The red stripes on the walls of the groove represent the absorbed fluence distribution from the threshold fluence ϕ_{th} at the edge of the groove to the fluence $\phi_{tip,n,j}$ at the tip of the groove. The cross section of the volume ablated during the n^{th} scan is highlighted by the orange hatched cross section. The incrementally increased depth of the groove is given by $z_{G,n}$, where n is the number of applied scans and $z_{S,n} = z_{G,n} - z_{G,n-1}$ is the incremental increase of the depth produced by the n^{th} scan along the groove.

The pulses of a Gaussian laser beam are irradiated onto the metal sample (the grey hatched cross section) at normal incidence (i.e. in z-direction). At the surface of the workpiece the transversal distribution of the incident fluence is shown by the red curve and defined by the beam radius w_0 and the pulse energy E_P (or peak fluence ϕ_0). Material removal by ablation on the surface occurs when the locally absorbed fluence exceeds the ablation threshold ϕ_{th}, which defines the width of the groove d_G by the doubled ablation radius r_{abl}. The model is based on the assumption that the groove depth $z_{G,n}$ after $n \in 1,2,\ldots N$ scans can be recursively calculated by

$$z_{\mathrm{G},n} = z_{\mathrm{G},n-1} + z_{\mathrm{S},n}, \tag{1}$$

where $z_{G,n-1}$ denotes the groove depth after n-1 scans and $z_{S,n}$ denotes the depth ablated by the n^{th} scan (cf. Fig 1). The depth $z_{S,n}$ ablated by the n^{th} scan corresponds to the accumulated depth ablated by the pulses with a spatial offset of δ_x during one scan.

It is noted that the model for the calculation of the depth progress only requires five generally known laser and scanning parameters. The required laser parameters are the pulse energy E_P, the repetition rate f_{rep}, the radius w_0 of the laser beam, the scanning speed v_x, and the number of scans n. The required material parameters are the absorptivity A, the energy penetration depth l_E, and the enthalpy h_V for heating and complete vaporisation of the material. The equations of the model in Holder et al., 2022 also demonstrate that the maximum achievable groove depth does neither depend on the repetition rate f_{rep} nor on the scanning parameters such as the scanning speed v_x and that - for a given beam radius w_0 and with the material-specific ablation threshold ϕ_{th} – it can only be increased by increasing the pulse energy E_P.

3. Experimental verification of the analytical model

In this study, the accuracy of the analytical model for predicting the dimensions of laser-ablated grooves was assessed by conducting experiments on different samples made of either the titanium alloy Ti6Al4V or the tungsten carbide cobalt composite WC-Co (WC 90%, Co 10%). The experimental setup is shown in Fig 2.

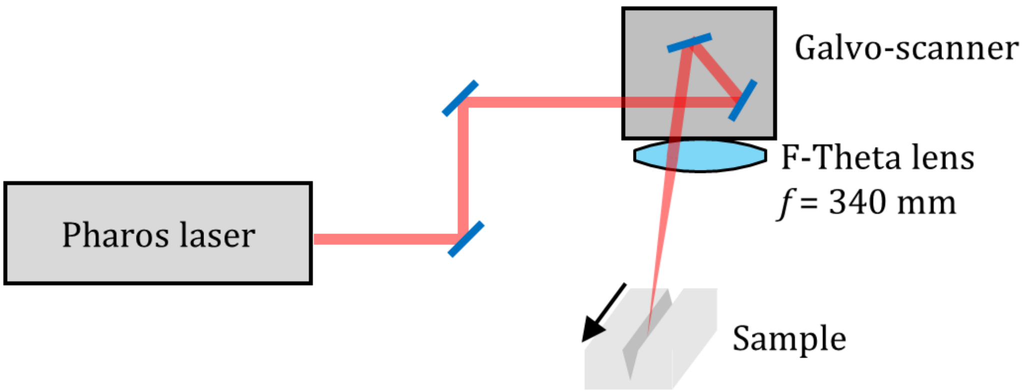

Fig. 2. Experimental setup used for laser ablation of grooves in metals with ultrashort laser pulses.

The experiments were performed using the laser system *Pharos* from *Light Conversion* with a wavelength of 1030 nm and an adjustable pulse duration τ_P between 260 fs and 15 ps. The laser beam had a Gaussian intensity distribution and was circularly polarized, with a beam propagation factor of $M^2 < 1.3$. The beam was focused onto the surface of the samples by an F-Theta lens with a focal length of 340 mm, resulting in a focal radius of w_0 = 55±5 µm. A Galvanometer-Scanner was used to scan the laser beam over the surface of the samples. The focus position was always set at the sample surface. Grooves of different lengths (ranging from 10 mm to 35 mm) were ablated in the samples with various pulse energies, repetition rates, scanning speeds, and numbers of scans, as summarized in Table 1.

Table 1. Sets of parameters as used for ablation of grooves with different depths and widths.

	Material	τ_P in fs	P_{av} in W	E_P in µJ	ϕ_0 in J/cm²	f_{rep} in kHz	v_x in m/s	δ_x in µm	Ω_x	Number of scans n
P1	Ti6Al4V	260	9.05	181	3.81	50	1.2	24	78%	300…10000
P2	Ti6Al4V	260	3.45	69	1.45	50	1.2	24	78%	300…10000
P3	Ti6Al4V	260	6.90	69	1.45	100	2.4	24	78%	600…20000
P4	Ti6Al4V	260	3.45	69	1.45	50	2.4	48	56%	600…20000
P5	Ti6Al4V	260	3.45	69	1.45	50	0.6	12	89%	150…5000
P6	WC-Co	1000	12.40	335	7.05	37	0.9	24	78%	150…10000
P7	WC-Co	1000	5.99	162	3.41	37	0.9	24	78%	150…10000

Cross sections were prepared by cutting perpendicular to the grooves (*y*-*z*-plane) after ablation and by grinding and polishing in order to investigate the shape of the grooves and measure their depth and width using an optical microscope. Fig 3 shows the cross sections obtained with the parameter set P1, P2 and P7 (cf. Table 1). The width of the groove remained constant at the value of about $d_\mathrm{G} = 113^{+4}_{-5}\ \mathrm{\mu m}$ and $d_\mathrm{G} = 138^{+8}_{-5}\ \mathrm{\mu m}$ for grooves machined in Ti6Al4V with E_P = 69 µJ and E_P = 181 µJ, respectively. The width of the groove also remained constant at $d_\mathrm{G} = 123^{+2}_{-2}\ \mathrm{\mu m}$ for the samples machined with E_P = 162 µJ in WC-Co. The V-shape clearly dominates the shape of the shown grooves for $n \geq 600$. he material parameters published by Kretsinger et al., 2013, Lickschat et al., 2020, and Lide and Haynes, 2010 were used for the calculation of the volume-specific enthalpy required to heat and vaporize the material. The calculation yielded a volume-specific enthalpy of h_V = 47 J/mm³ for titanium and h_V = 55 J/mm³ for tungsten carbide. The absorptivity at normal incidence and at a wavelength of about 1 µm was set to A = 0.51 for titanium as published by Palm et al., 2018 and 0.54 for tungsten carbide as published by Lickschat et al., 2020. The effective penetration depth was used as a fit parameter. A good agreement between the calculated and the experimental results was found with l_E = 30 nm for Ti6Al4V and l_E = 22 nm for WC-Co. The fitted values are consistent with the experimentally determined values between 26 nm and 30 nm for titanium / Ti6Al4V from Maharjan et al., 2018 and Mannion et al., 2004 and with the experimentally determined values between 19 nm and 23 nm for tungsten carbide from Meliani et al., 2021 and Pfeiffer et al., 2011.

The calculation of the groove widths for the peak fluences of 3.81 J/cm² (P1) and 1.45 J/cm² (P2) for Ti6Al4V yield d_G = 126 µm and d_G = 100 µm, respectively. The experimentally determined widths of $d_\mathrm{G} = 138^{+8}_{-5}\ \mathrm{\mu m}$ (P1) and $d_\mathrm{G} = 113^{+4}_{-5}\ \mathrm{\mu m}$ (P2) are slightly larger. For WC-Co, the groove widths for the peak fluences of 7.05 J/cm² (P6) and 3.41 J/cm² (P7) yield d_G = 144 µm and d_G = 128 µm, respectively. Again, the experimentally determined widths of $d_\mathrm{G} = 153^{+3}_{-3}\ \mathrm{\mu m}$ (P6) and $d_\mathrm{G} = 123^{+2}_{-2}\ \mathrm{\mu m}$ (P7) are close to the calculated values. The moderate deviations of less than 15% may be explained by the fact that no incubation effect is taken into account in the model, as described by in Holder et al., 2022.

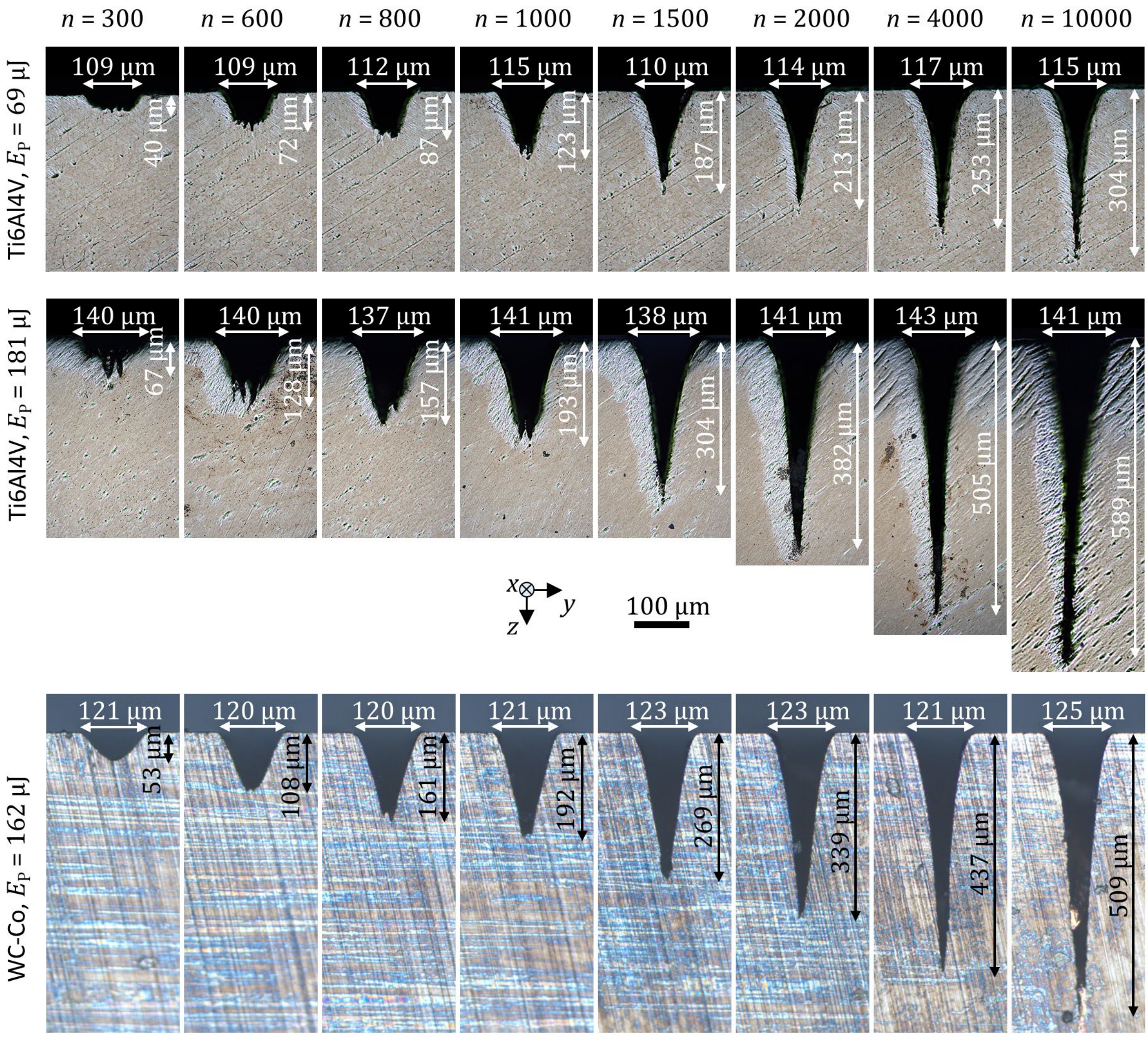

Fig. 3. Cross sections of grooves ablated in Ti6Al4V with the parameter set P1. The depth and width of each groove is indicated by a yellow double arrow and a green double arrow, respectively.

The progress of the groove depth $z_{G,n}$ as a function of the number n of scans was recursively calculated according to the model described in Holder et al., 2022. The results of the calculations are compared to the experimental results in Fig 4. The groove depths as calculated by the model presented in Holder et al., 2022 and as measured from the cross sections for the different parameter combinations P1 to P7 (cf. Fig 4) are represented in different colours with solid lines and data points, respectively.

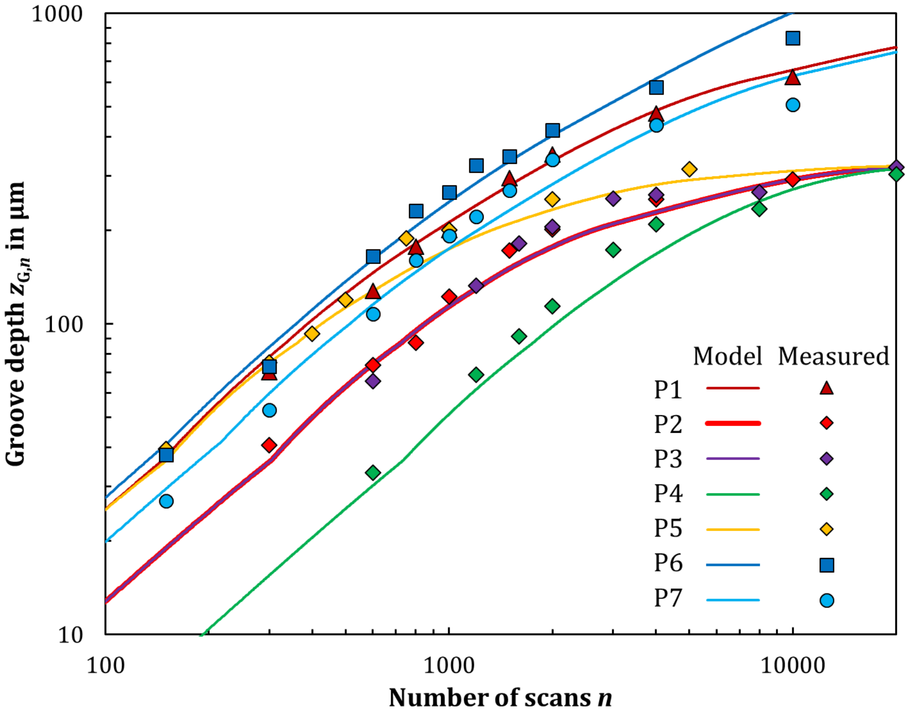

Fig. 4. Calculated groove depth (dotted lines, “Model”) and measured groove depth (data points, “Measured”) as a function of the number of scans for laser ablated grooves in Ti6Al4V and WC-Co using the different parameter sets as given in Table 1.

The relationship between the groove depth and the number of scans was found to be almost linear up to an aspect ratio of approximately 1.5 for both materials. For higher aspect ratios, the progress of the depth slows down. Increasing pulse energy resulted in higher depth progress and deeper grooves at constant repetition rate and scanning speed (cf. P1 and P2), while constant pulse energy and overlap produced similar groove depth for different numbers of scans (cf. P2 and P3). However, the net processing time was halved for double scanning speed at a twofold repetition rate. The highest depth progress was achieved with lower scanning speeds for constant pulse energy and repetition rate (cf. P3, P4 and P5). The highest groove depth achieved for Ti6Al4V was 624 µm with the highest pulse energy and number of scans (P1). As expected, an increasing pulse energy also resulted in higher depth progress and deeper grooves for samples made from WC-Co (cf. P6 and P7).

The groove depths as calculated by the model (dotted lines, “Model”) and as measured by the cross sections with the optical microscope (data points, “Measured”) are in very good agreement for the different parameter combinations, for the different number of scans, and for both processed materials.

Knowing the laser parameters E_P and f_{rep}, the scanning speed v_x and beam radius w_0, and the three material parameters A, l_E and h_V, the model allows for the prediction of the groove dimensions as a function of the number of scans n and the maximum achievable groove depth.

4. Conclusion

The predictions of the analytical model developed in Holder et al., 2022 agree well with the experimental results regarding the depth and width of V-shaped grooves, which were machined in metals by means of ultrashort laser pulses. The model takes into account various laser, scanning, and material parameters and has been experimentally validated using samples made from Ti6Al4V or WC-Co and for grooves with a depth of up to 833 µm. The model is a valueable tool for designing ablation processes regarding groove dimensions, for determining process windows with a high depth progress, and for identifying the maximum achievable groove depth.

Acknowledgements

This work was funded by the Federal Ministry for Economic Affairs and Climate Action (BMWK) in the frame of the projects “BionicTools” (03EN4007G) and “DigiTain” (19S22006Z). The authors wish to thank Ulrich Höchner and Light Conversion for providing the Pharos laser. Furthermore, the authors wish to thank Kim Glumann and Nils Ensminger for the support with the experiments.

References

Holder, D., Weber, R., Graf, T., 2022. Analytical Model for the Depth Progress during Laser Micromachining of V-Shaped Grooves. Micromachines 13 (870).

Holder, D., Weber, R., Graf, T., Onuseit, V., Brinkmeier, D., Förster, D.J., Feuer, A., 2021. Analytical model for the depth progress of percussion drilling with ultrashort laser pulses. Appl. Phys. A 127 (5). doi:10.1007/s00339-021-04455-3.

Kretsinger, R.H., Uversky, V.N., Permyakov, E.A., 2013. Encyclopedia of Metalloproteins. Springer New York, New York, NY, 134 pp.

Lickschat, P., Metzner, D., Weißmantel, S., 2020. Fundamental investigations of ultrashort pulsed laser ablation on stainless steel and cemented tungsten carbide. The International Journal of Advanced Manufacturing Technology 109, 1167–1175.

Lide, D.R., Haynes, W.M., 2010. CRC Handbook of Chemistry and Physics, 90th ed. CRC Press/Taylor and Francis, Boca Ranton, FL, USA, 2760 pp.

Maharjan, N., Zhou, W., Zhou, Y., Guan, Y., 2018. Ablation morphology and ablation threshold of Ti-6Al-4V alloy during femtosecond laser processing. Appl. Phys. A 124 (8). doi:10.1007/s00339-018-1928-3.

Mannion, P.T., Magee, J., Coyne, E., O'Connor, G.M., Glynn, T.J., 2004. The effect of damage accumulation behaviour on ablation thresholds and damage morphology in ultrafast laser micro-machining of common metals in air. Applied Surface Science 233, 275–287. doi:10.1016/j.apsusc.2004.03.229.

Meliani, H., Assoul, M., Fontaine, M., Malkhasyan, V., Gilbin, A., Monteil, G., 2021. Femtosecond laser–matter interaction of tungsten carbide. Applied Optics 60 (3), 2021.

Palm, K.J., Murray, J.B., Narayan, T.C., Munday, J.N., 2018. Dynamic Optical Properties of Metal Hydrides. ACS Photonics 5, 4677–4686.

Pfeiffer, M., Engel, A., Weißmantel, S., Scholze, S., Reisse, G., 2011. Microstructuring of Steel and Hard Metal using Femtosecond Laser Pulses. Physics Procedia 12, 60–66. doi:10.1016/j.phpro.2011.03.106.